

Estimation of the spatial decoherence time in circular quantum dots

Michael Genkin, Erik Waltersson, and Eva Lindroth

Atomic Physics, Stockholm University, AlbaNova, S-10691 Stockholm, Sweden

(Received 11 February 2009; revised manuscript received 6 May 2009; published 16 June 2009)

We propose a simple phenomenological model to estimate the spatial decoherence time in quantum dots. The dissipative phase-space dynamics is described in terms of the density matrix and the corresponding Wigner function, which are derived from a master equation with Lindblad operators linear in the canonical variables. The formalism was initially developed to describe diffusion and dissipation in deep inelastic heavy-ion collisions, but an application to quantum dots is also possible. It allows us to study the dependence of the decoherence rate on the dissipation strength, the temperature, and an external magnetic field, which is demonstrated in illustrative calculations on a circular GaAs one-electron quantum dot.

DOI: [10.1103/PhysRevB.79.245310](https://doi.org/10.1103/PhysRevB.79.245310)

PACS number(s): 73.21.La, 03.65.Yz

I. INTRODUCTION

Decoherence processes in semiconductor quantum dots have attracted a lot of interest in the last years not only due to their relevance for a quantum computer implementation¹ but also because they present an experimentally accessible system to study the decoherence process in general.²⁻⁶ As demonstrated in several theoretical works,⁷⁻²⁶ there are different processes that can lead to decoherence in a quantum dot, such as interaction with optical and acoustic phonons or hyperfine interactions, in particular, through electron-spin coupling to a bath of nuclear spins. The processes occur on different time scales and are sensitive to external parameters such as temperature or external magnetic fields. The coupling to the environment can be treated within the Born-Markov approximation,^{10,18,21} but also effects beyond the Markovian limit can play a role.^{12,15-17,20,26} However, the vast majority of the processes studied so far focuses on spin decoherence, mainly, because it is the spin of the electron(s) that makes a quantum computational application of quantum dots possible.¹ Nevertheless, also the spatial decoherence which is arising from dissipative phase-space dynamics in the canonically conjugated coordinates and momenta (see, e.g., Ref. 27 for a detailed discussion) can possibly become relevant. As an example, one can think of a situation where the space and spin parts of a wave function are connected by the fermionic total asymmetry condition. Also in such a scheme as recently suggested in Ref. 28, where electromagnetic transitions in solid-state devices are used for controlled operations, phase-space dynamics can be important since it is not only the spin but also the total angular momentum that plays a crucial role.

In the present work, we aim to estimate the spatial decoherence time scale and to study its dependence on the coupling strength to the environment, on the temperature, and on an external magnetic field. The latter plays a role since it determines the cyclotron frequency and hence also the effective confinement strength, which, together with the temperature, was shown to influence the asymptotic spatial decoherence in quadratic potentials.²⁹ In addition, the magnetic field also explicitly influences the time evolution of the system.

The study is carried out using an analytical model in the Markovian limit with linear Lindblad operators, which was

initially developed to study diffusion and dissipation in heavy-ion collisions.^{30,31} We show that with an appropriate choice of the involved constants, the model can also be used to describe a two-dimensional quantum dot in a perpendicularly applied external magnetic field (Sec. II). The temperature dependence is incorporated in the diffusion coefficients which significantly determine the time behavior of the density matrix.³² The model has the advantage that it is rather general and allows us to include environmental effects without the necessity to explicitly compute the system-environment interaction. The latter is instead taken into account by phenomenological constants that emerge from the Lindblad operators. This is sometimes referred to as the reduced dynamics approach. In practical calculations, it is then only necessary to find appropriate values for these constants, depending on the environmental effects one wishes to consider. In the illustrative calculations shown here, we relate these effects to the electron-phonon interaction, but one could also consider other effects within basically the same model without loss of generality provided the required input (as, e.g., electron-phonon scattering rates, in our case) is known at least approximately. In Sec. III, we discuss how the decoherence time scale can be determined from the model, using the general results derived in Ref. 31. It is demonstrated in more detail in illustrative calculations on a circular GaAs one-electron quantum dot in Sec. IV followed by a discussion and concluding remarks in Sec. V.

II. DESCRIPTION OF THE MODEL

The Hamiltonian of a one-electron quantum dot with a harmonic confinement (which is a very common choice; see, e.g., Refs. 33-36) in the xy plane and exposed to an external magnetic field B pointing in the z direction reads as

$$H = \frac{\mathbf{p}^2}{2m^*} + \frac{1}{2}m^*\omega_0^2r^2 + \frac{e^2}{8m^*}B^2r^2 + \frac{e}{2m^*}BL_z + g^*\mu_bBS_z. \quad (1)$$

Here, ω_0 denotes the confinement strength, $r = \sqrt{x^2 + y^2}$ is the radial polar coordinate, L_z and S_z denote the z component of the orbital-angular-momentum operator and spin operator, respectively, μ_b is the Bohr magneton, and m^*, g^* are the

effective mass and effective g factor for the used semiconductor. By defining the cyclotron frequency $\omega_c = eB/m^*$ and the effective frequency $\omega = \sqrt{\omega_0^2 + \omega_c^2}/4$, it can be written as

$$H = H_0 + H_s, \quad (2)$$

where $H_s = g^* \mu_b B S_z$ is the spin part and

$$H_0 = \frac{\mathbf{p}^2}{2m^*} + \frac{1}{2}m^*\omega^2 r^2 + \frac{e}{2m^*}BL_z. \quad (3)$$

The latter expression is a general Hamiltonian of a two-dimensional harmonic oscillator exposed to a perpendicular magnetic field. The phase-space dynamics of such a system when coupled to the environment was, for example, studied semiclassically in Ref. 37 by means of a Fokker-Planck equation. Also an explicit inclusion of a heat bath in this Hamiltonian is possible, which leads to non-Markovian dynamics as recently demonstrated in Ref. 38 for a nuclear system. Another possible approach is the influence functional method,³⁹ which was used to study the decoherence dynamics of two coupled harmonic oscillators in a general environment, with their potential minima being separated by a finite distance.⁴⁰ Here, however, we will adopt a simpler phenomenological picture to describe the quantum-dot coupling to an external environment based on a Markovian master equation⁴¹ which is known to be valid in the weak-coupling limit.⁴² In this framework, dissipation and decoherence are described by Lindblad operators, which is a rather common approach.^{29,43–47} The formalism is based on an earlier work of Gupta *et al.*³⁰ and Sandulescu *et al.*³¹ which is briefly introduced below.

Due to the excitation of internal degrees of freedom (i.e., the nucleons) in heavy-ion collisions, dissipation is a rather important issue in its quantum-mechanical description. It is common to describe such a dynamics in terms of dimensionless coordinates of proton and neutron asymmetry defined as $q_1 = (Z_1 - Z_2)/(Z_1 + Z_2)$, $q_2 = (A_1 - A_2)/(A_1 + A_2)$, where Z_1, Z_2 and A_1, A_2 are the charges and masses of the colliding nuclei. A model to couple these coordinates was suggested in Ref. 30. Later, this model was generalized in Ref. 31, where the complete description of the dissipative dynamics was explicitly derived from the Markovian master equation for the density matrix ρ given below,

$$\frac{d\rho}{dt} = -\frac{i}{\hbar}[H, \rho] + \frac{1}{2\hbar} \sum_j ([V_j \rho, V_j^\dagger] + [V_j, \rho V_j^\dagger]), \quad (4)$$

where V_j is a set of Lindblad operators, and the considered Hamiltonian had the following form:

$$H = \sum_{k=1}^2 \left(\frac{1}{2m_k} p_k^2 + \frac{m_k \omega_k^2}{2} q_k^2 \right) + \frac{1}{2} \sum_{k_1, k_2=1}^2 \mu_{k_1 k_2} (p_{k_1} q_{k_2} + q_{k_2} p_{k_1}) + \nu_{12} q_1 q_2 + \kappa_{12} p_1 p_2. \quad (5)$$

Here, p_1, p_2 are the canonically conjugated momenta to the charge and mass asymmetry coordinates. The appearing coupling constants can be partly calculated from the nuclear liquid-drop model or determined by fitting to experimental data. However, if these constants are chosen as $\nu_{12}=0$, $\kappa_{12}=0$, $\mu_{11}=0$, and $\mu_{22}=0$ and

$$q_1 = x, \quad q_2 = y, \quad p_1 = p_x, \quad p_2 = p_y, \quad m_1 = m^* = m_2,$$

$$\omega_1 = \omega = \omega_2, \quad \mu_{21} = \frac{eB}{2m^*} = -\mu_{12}, \quad (6)$$

the Hamiltonian H_0 from Eq. (3) is reproduced exactly. Moreover, following the same choice of linear Lindblad operators as in Ref. 31:

$$V_j = \sum_{k=1}^2 (a_{jk} p_k + b_{jk} q_k), \quad j = 1, 2, 3, 4, \quad (7)$$

where a_{jk}, b_{jk} are complex numbers, we see that the spin part H_s of the full quantum-dot Hamiltonian (2) commutes with the full Hamiltonian as well as with the Lindblad operators so that the resulting equations of motion of the first and second moments in the canonical variables are unaffected. In other words, all results derived in Ref. 31 also remain valid in our case. Thus, we will omit the derivation, solution, and discussion of the equations of motion here and only briefly quote the main results relevant for our study. At this point, we would also like to mention that since the spin motion decouples, no spin dephasing effects are present in the spatial decoherence studied here. The spin relaxation and dephasing times (often called T_1 and T_2) can also be studied within an equations-of-motion approach (see, e.g., Ref. 20 and the references within), which, however, requires different models and is not considered in the present work.

We use the abbreviations

$$\mathbf{m}(t) = (\langle x \rangle, \langle y \rangle, \langle p_x \rangle, \langle p_y \rangle)^T \quad (8)$$

for the time-dependent expectation values of the canonical phase-space operators and

$$\sigma(t) = \begin{pmatrix} \sigma_{xx} & \sigma_{xy} & \sigma_{xp_x} & \sigma_{xp_y} \\ \sigma_{yx} & \sigma_{yy} & \sigma_{yp_x} & \sigma_{yp_y} \\ \sigma_{p_x x} & \sigma_{p_x y} & \sigma_{p_x p_x} & \sigma_{p_x p_y} \\ \sigma_{p_y x} & \sigma_{p_y y} & \sigma_{p_y p_x} & \sigma_{p_y p_y} \end{pmatrix} \quad (9)$$

for the time-dependent symmetric covariance matrix, where the elements are defined as

$$\sigma_{AB} = \sigma_{BA} = \frac{1}{2} \langle AB + BA \rangle - \langle A \rangle \langle B \rangle \quad (10)$$

for any two operators A, B . The time evolution of the expectation values is given by

$$\mathbf{m}(t) = \exp(tY) \mathbf{m}(0), \quad (11)$$

where $\mathbf{m}(0)$ denotes the initial expectation values and Y is the time-evolution matrix which, after insertion of the constants given in Eq. (6) into the general result from Ref. 31, becomes

$$Y = \begin{pmatrix} -\lambda_{11} & -\lambda_{12} - eB/(2m^*) & 1/m^* & -\alpha_{12} \\ -\lambda_{21} + eB/(2m^*) & -\lambda_{22} & \alpha_{12} & 1/m^* \\ -m^*\omega^2 & \beta_{12} & -\lambda_{11} & -\lambda_{21} - eB/(2m^*) \\ -\beta_{12} & -m^*\omega^2 & -\lambda_{12} + eB/2m & -\lambda_{22} \end{pmatrix}. \quad (12)$$

The phenomenological dissipation constants λ_{kl} , α_{12} and β_{12} emerge from the Lindblad operators in Eq. (7) and are explicitly given by

$$\begin{aligned} \alpha_{12} &= -\text{Im}\langle \mathbf{a}_1, \mathbf{a}_2 \rangle, \\ \beta_{12} &= -\text{Im}\langle \mathbf{b}_1, \mathbf{b}_2 \rangle, \\ \lambda_{kl} &= -\text{Im}\langle \mathbf{a}_k, \mathbf{b}_l \rangle, \end{aligned} \quad (13)$$

where the vectors $\mathbf{a}_k, \mathbf{b}_l$ are defined as [cf. Eq. (7)]

$$\mathbf{a}_k = (a_{1k}, a_{2k}, a_{3k}, a_{4k})^T, \quad \mathbf{b}_k = (b_{1k}, b_{2k}, b_{3k}, b_{4k})^T, \quad (14)$$

with the scalar product

$$\langle \mathbf{x}, \mathbf{y} \rangle = \sum_{i=1}^4 x_i^* y_i. \quad (15)$$

However, since we consider a circular one-electron quantum dot where the dynamics is symmetric in x and y , we set the off-diagonal dissipation constants to be zero here and in the following (i.e., $\lambda_{12}=0=\lambda_{21}$ and $\alpha_{12}=0=\beta_{12}$) and, furthermore, demand $\lambda_{11}=\lambda_{22}\equiv\lambda$, hereby restricting the dissipation strength to a single phenomenological parameter. For the covariance matrix, the following time evolution is derived

$$\sigma(t) = \exp(tY)[\sigma(0) - \sigma(\infty)][\exp(tY)]^T + \sigma(\infty). \quad (16)$$

Here, $\sigma(0)$ is the initial covariance matrix and $\sigma(\infty)$ its asymptote. The latter can be determined from a set of diffusion coefficients, which are given by

$$\begin{aligned} D_{p_k p_l} &= D_{p_l p_k} = \frac{\hbar}{2} \text{Re}\langle \mathbf{b}_k, \mathbf{b}_l \rangle, \\ D_{q_k q_l} &= D_{q_l q_k} = \frac{\hbar}{2} \text{Re}\langle \mathbf{a}_k, \mathbf{a}_l \rangle, \\ D_{q_k p_l} &= D_{p_l q_k} = -\frac{\hbar}{2} \text{Re}\langle \mathbf{a}_k, \mathbf{b}_l \rangle, \end{aligned} \quad (17)$$

where the notation $q_1=x, q_2=y, p_1=p_x, p_2=p_y$ is used. They are connected to the asymptotic covariance matrix by the relation

$$Y\sigma(\infty) + \sigma(\infty)Y^T = -2D, \quad (18)$$

where D is the symmetric diffusion matrix

$$D = \begin{pmatrix} D_{xx} & D_{xy} & D_{xp_x} & D_{xp_y} \\ D_{yx} & D_{yy} & D_{p_x y} & D_{p_y y} \\ D_{p_x x} & D_{p_x y} & D_{p_x p_x} & D_{p_x p_y} \\ D_{p_y x} & D_{p_y y} & D_{p_y p_x} & D_{p_y p_y} \end{pmatrix}. \quad (19)$$

The choice of the diffusion coefficients is, in general, a non-trivial issue since there are several conditions that have to be obeyed in order to preserve the non-negativity of the density matrix and the uncertainty relation. This will not be discussed here (see, e.g., Refs. 32 and 48–51 for more details). In the present work, we use a two-dimensional extension of the commonly used temperature-dependent coefficients of a harmonic oscillator without further mixing, such that the diffusion matrix is diagonal,

$$\begin{aligned} D_{xx} &= \frac{\hbar\lambda}{2m^*\omega} \coth\left(\frac{\hbar\omega}{2kT}\right) = D_{yy}, \\ D_{p_x p_x} &= \frac{\hbar\lambda m^*\omega}{2} \coth\left(\frac{\hbar\omega}{2kT}\right) = D_{p_y p_y}, \end{aligned} \quad (20)$$

and $D_{ij}=0$ otherwise, where T is the temperature and k is the Boltzmann constant. From the given time evolution of the first and second moments, one can obtain the Wigner function f_W of the system, which is the best possible quantum-mechanical analogon to a classical phase-space density (although it is, in general, not positive everywhere and, therefore, cannot be interpreted as a true density). The latter was found by means of Weyl operators in Ref. 31,

$$\begin{aligned} f_W(x, y, p_x, p_y, t) &= \frac{1}{\sqrt{\det[2\pi\sigma(t)]}} \\ &\times \exp\left\{-\frac{1}{2}[\xi - \mathbf{m}(t)]^T \sigma(t)^{-1} [\xi - \mathbf{m}(t)]\right\}, \end{aligned} \quad (21)$$

where $\xi=(x, y, p_x, p_y)^T$ is the phase-space vector. This agrees with the result obtained in an earlier work.^{37,52,53} In the following, we use this result to calculate the decoherence rate.

III. DECOHERENCE RATE

It is by far not trivial to give a general definition of “decoherence.” Often, it is simply referred to as “loss of coherence” in a quantum system or as the entanglement of the latter with its environment. Technically, however, the degree of decoherence can be expressed through the density matrix of a quantum system or, more precisely, through the damping

of its off-diagonal elements.^{29,44,54–56} We shall adopt this definition in the following, although it is also possible to study decoherence directly in terms of the Wigner function.⁵⁷ The density matrix is connected to the Wigner function by the transformation

$$\begin{aligned} \langle x,y|\rho|x',y'\rangle(t) &= \int \int dp_x dp_y \\ &\times \exp\left\{\frac{i}{\hbar}[p_x(x-x') + p_y(y-y')]\right\} \\ &\times f_W[(x+x')/2, (y+y')/2, p_x, p_y, t], \end{aligned} \quad (22)$$

which can be carried out analytically for the Wigner function (21). After evaluating the two-dimensional Gaussian integral and introducing new coordinates,

$$\begin{aligned} \Sigma_x &= \frac{x+x'}{2}, \quad \Delta_x = x-x', \\ \Sigma_y &= \frac{y+y'}{2}, \quad \Delta_y = y-y', \end{aligned} \quad (23)$$

we arrive at the following expression:

$$\begin{aligned} \langle x,y|\rho|x',y'\rangle(t) &= N \exp\left[-K_1(\Sigma_x - \langle x \rangle)^2 - K_2(\Sigma_y - \langle y \rangle)^2 \right. \\ &- K_3(\Sigma_x - \langle x \rangle)(\Sigma_y - \langle y \rangle) - K_4\Delta_x^2 - K_5\Delta_y^2 \\ &+ K_6\Delta_x\Delta_y + iK_7(\Sigma_x - \langle x \rangle)\Delta_x + iK_8 \\ &\times (\Sigma_y - \langle y \rangle)\Delta_y + iK_9(\Sigma_x - \langle x \rangle)\Delta_y + iK_{10} \\ &\left. \times (\Sigma_y - \langle y \rangle)\Delta_x + \frac{i}{\hbar}(\langle p_x \rangle \Delta_x + \langle p_y \rangle \Delta_y)\right]. \end{aligned} \quad (24)$$

The normalization factor is given by

$$N = \sqrt{\frac{4\pi^2}{\det[2\pi\sigma(t)](c_{33}c_{34} - c_{34}^2)}}, \quad (25)$$

where $c_{ij}=c_{ji}$ denote the elements of the inverse of the covariance matrix $\sigma(t)^{-1}$. The explicit form of the time-dependent constants $K_1(t), \dots, K_{10}(t)$ in terms of the matrix elements $c_{ij}(t)$ is given below

$$K_1(t) = \frac{c_{11}}{2} + \frac{c_{13}c_{14}c_{34} - \frac{1}{2}(c_{13}^2c_{44} + c_{14}^2c_{33})}{c_{33}c_{44} - c_{34}^2},$$

$$K_2(t) = \frac{c_{22}}{2} + \frac{c_{23}c_{24}c_{34} - \frac{1}{2}(c_{23}^2c_{44} + c_{24}^2c_{33})}{c_{33}c_{44} - c_{34}^2},$$

$$K_3(t) = c_{12} + \frac{c_{34}(c_{13}c_{24} + c_{14}c_{23}) - (c_{13}c_{23}c_{44} + c_{14}c_{24}c_{33})}{c_{33}c_{44} - c_{34}^2},$$

$$K_4(t) = \frac{c_{44}}{2\hbar^2(c_{33}c_{44} - c_{34}^2)},$$

$$K_5(t) = \frac{c_{33}}{2\hbar^2(c_{33}c_{44} - c_{34}^2)},$$

$$K_6(t) = \frac{c_{34}}{\hbar^2(c_{33}c_{44} - c_{34}^2)},$$

$$K_7(t) = \frac{c_{34}c_{14} - c_{44}c_{13}}{\hbar(c_{33}c_{44} - c_{34}^2)},$$

$$K_8(t) = \frac{c_{34}c_{23} - c_{24}c_{33}}{\hbar(c_{33}c_{44} - c_{34}^2)},$$

$$K_9(t) = \frac{c_{34}c_{13} - c_{14}c_{33}}{\hbar(c_{33}c_{44} - c_{34}^2)},$$

$$K_{10}(t) = \frac{c_{34}c_{24} - c_{23}c_{44}}{\hbar(c_{33}c_{44} - c_{34}^2)}. \quad (26)$$

Note that also the expectation values are functions of time governed by Eq. (11). In the particular case of a circular one-electron quantum dot, the dynamics is considerably simplified due to the symmetry in x and y because the dispersions of the terms quadratic in Σ_x, Σ_y that determine the damping of the diagonal elements of the density matrix are identical ($K_1=K_2$). The same holds for the dispersions of the terms quadratic in Δ_x, Δ_y that describe the damping of the off-diagonal elements ($K_4=K_5$), which, following Refs. 29 and 54–56, allows us to define a single decoherence parameter

$$\delta_D(t) = \frac{1}{2} \sqrt{\frac{K_1}{K_4}} = \frac{1}{2} \sqrt{\frac{K_2}{K_5}}. \quad (27)$$

The definition is such that $\delta_D=1$ corresponds to a perfectly coherent state and $\delta_D=0$ implies that coherence is lost. In the next section, we investigate its time behavior under the influence of the magnetic field, the temperature, and dissipation. At this point, we would like to emphasize that not only the decoherence degree but also other purely quantum-mechanical quantities can be extracted from the Wigner function in the case studied here. If the quantum dot is prepared in a coherent state, the Wigner function is positive everywhere and hence it coincides with the classical phase-space density.⁵⁸ For example, the quantum-mechanical probability density $\rho(x, y, t)$ is directly obtained from the Wigner function by setting $x=x', y=y'$ (i.e., $\Sigma_x=x, \Sigma_y=y, \Delta_x=0=\Delta_y$) in Eq. (24).

IV. ILLUSTRATIVE CALCULATIONS

As an illustration, we consider a one-electron GaAs-quantum dot. Throughout this section, we use effective atomic units, i.e., atomic units scaled with the GaAs material parameters $\epsilon_r=12.4$ (dielectric constant) and $m^*=0.067m_e$, where m_e is the electron mass, and a confinement strength of $\hbar\omega_0=5$ meV. Disregarding the spin part which, as previously mentioned, is irrelevant for the phase-space dynamics

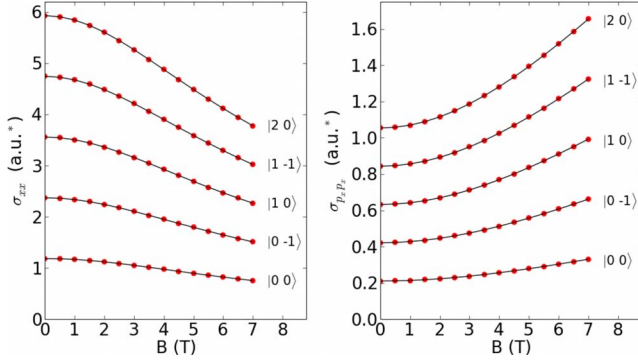


FIG. 1. (Color online) Variances in position and momentum shown for some one-electron GaAs quantum-dot states $|nm\rangle$ given in effective atomic units: σ_{xx} has dimension length², where the length is measured in effective Bohr radii ($a_0^* \approx 9.794$ nm) and $\sigma_{p_x p_x}$ is measured in Hartree^{*} m^* , where $m^* = 0.067m_e$ and Hartree^{*} ≈ 11.857 meV is the effective atomic energy unit.

studied here, the solutions to the Hamiltonian (3) can be written in terms of a principal and an angular quantum number

$$\psi_{nm}(r, \varphi) = u_{nm}(r)e^{im\varphi}. \quad (28)$$

Since we consider the system to be initially in a prepared state, the initial conditions required for the time evolution of the first and second moments [Eqs. (11) and (16)] are, unless given analytically, calculated numerically for any state in Eq. (28) using a B -spline basis⁵⁹ as demonstrated in Ref. 35. In particular, we have $\mathbf{m}(0)=0$ for the expectation values of x, y, p_x, p_y and the initial covariance matrix has the following form:

$$\sigma(0) = \begin{pmatrix} \sigma_{xx} & 0 & 0 & m\hbar \\ 0 & \sigma_{yy} & -m\hbar & 0 \\ 0 & -m\hbar & \sigma_{p_x p_x} & 0 \\ m\hbar & 0 & 0 & \sigma_{p_y p_y} \end{pmatrix}, \quad (29)$$

where $\sigma_{xx} = \sigma_{yy}$ and $\sigma_{p_x p_x} = \sigma_{p_y p_y}$ (the equality is again a consequence of the symmetry) are numerically calculated values. They depend on the effective confinement frequency and therefore on the magnetic field since it influences the latter ($\omega = \sqrt{\omega_0^2 + \omega_c^2}/4$, where $\omega_c = eB/m^*$, cf. Sec. II). The explicit dependence is illustrated in Fig. 1.

This behavior can be understood qualitatively by considering a usual one-dimensional harmonic oscillator, where the variances of the n th state are given by $\sigma_{xx} = (1+2n)\hbar/(2m^*\omega)$ and $\sigma_{p_x p_x} = (1+2n)\hbar m^*\omega/2$. Physically, this simply means that with increasing magnetic field, the electron becomes more localized in position space and less localized in momentum space. The uncertainty relation in each coordinate, however, does not depend on ω (and hence neither on the magnetic field) since it is determined by the product of the variances,

$$\sigma_{xx}\sigma_{p_x p_x} - \sigma_{xp_x}^2 \geq \frac{1}{4} \quad (30)$$

(and in the same way for y, p_y). Also, for the quantum-dot states, the initial covariances σ_{xp_x} and σ_{yp_y} always vanish. Among all states, it is only the ground state $|nm\rangle = |00\rangle$ that has minimum uncertainty due to its ideal Gaussian shape, while for excited states the Gaussian shape is disturbed and the uncertainty relation becomes a strict inequality. This corresponds to the fact that the ground state of a harmonic oscillator is a particular case of a Glauber coherent state. Hence, $\delta_D(t=0)$ must be equal to unity for the quantum-dot ground state which agrees with the calculations and retrospectively confirms the imposed definition of the decoherence parameter.

In addition to the previously discussed initial conditions, also the coupling strength to the environment needs to be determined. As already mentioned in the introduction, the advantage of the model used here is that one can phenomenologically account for, in principle, any kind of environmental effects simply by choosing appropriate values of the phenomenological constants. However, since the master equation (4) is only valid for weak coupling of the reduced system to the environment, the ratio λ/ω should be much smaller than unity, which restricts the model to the description of processes that obey this condition. Here, we consider the dissipative effects to be caused by electron-phonon interactions and therefore the dissipation rate λ is approximately given by the electron-phonon scattering rate. The latter ones were found to be typically on the order of $\lambda \approx 10$ ns⁻¹ in GaAs structures.⁶⁰⁻⁶³ For the effective confinement strength chosen here, this yields $\lambda \approx 10^{-3}\omega$ and hence the Markovian approach can be seen as justified in the present study. Another aspect to be considered is that apart from being incorporated in the diffusion coefficients [Eq. (20)], the temperature also influences the phonon-scattering rate. However, since the phonon-scattering rates for different temperatures are not known exactly, the parameter λ is varied independently in the relevant region at different temperatures to investigate its influence on the decoherence time scale.

Figure 2 shows the time evolution of the probability density [obtained by setting $x=x', y=y'$ in Eq. (24)] and Fig. 3 shows the time evolution of the decoherence degree when the quantum dot is initially prepared in the ground state. We observe that the asymptotic degree of decoherence strongly depends on the temperature and, more weakly, on the magnetic-field strength. Naturally, higher temperatures lead to stronger decoherence, while a strong magnetic field has a protective effect on quantum coherence. This corresponds to the result obtained for the one-dimensional case,²⁹ where the asymptotic decoherence degree was shown to be $\delta_D(\infty) = \tanh[\hbar\omega/(2kT)]$ (recall that the effective confinement ω increases with B). However, the time scale itself on which the system approaches its asymptotical decoherence is determined by the coupling to the environment. Depending on the latter, decoherence occurs on a time scale between 20 and 200 ps. It is interesting to note that the rule of thumb to estimate the ratio of relaxation (τ_r) and decoherence (τ_D) time scale⁵⁵

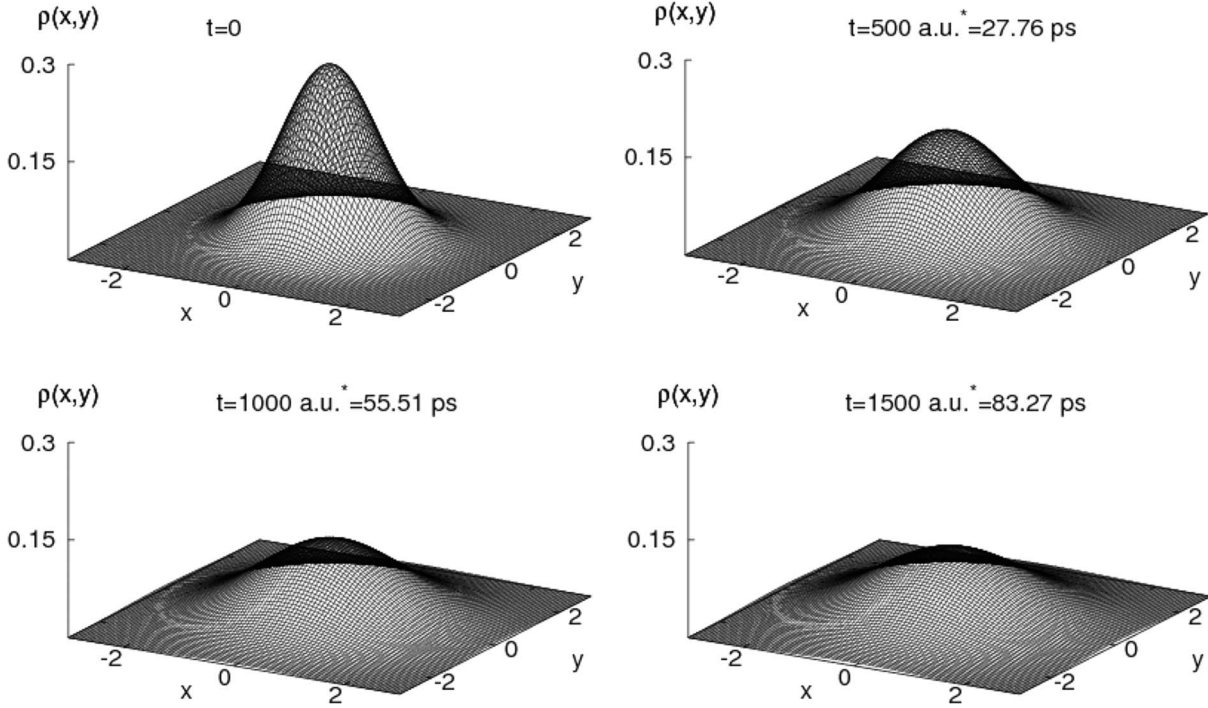


FIG. 2. Time evolution of the probability density in the coordinate space shown for $B=1$ T, $T=25$ K, and $\lambda=10^{-3}\omega$ where the dot is initially prepared in the ground state. The coordinates are given in effective Bohr radii $a_0^* \approx 9.794$ nm and the probability density in units of $1/(a_0^*)^2$.

$$\frac{\tau_r}{\tau_D} \approx \left(\frac{\sqrt{\sigma_{xx}}}{L_{dB}} \right)^2, \quad (31)$$

where L_{dB} is the thermal de Broglie wavelength,

$$L_{dB} = \frac{\hbar}{\sqrt{2m^*kT}} \quad (32)$$

holds in the case studied here, but the ratio is on the order of unity, which is a rather untypical behavior. In fact, in many situations decoherence is several orders of magnitude faster than dissipation and relaxation. For macroscopic systems, the

ratio in Eq. (31) becomes astronomically large.^{29,55,64} In quantum dots, however, the wave-packet spread can be on the same order as the thermal de Broglie wavelength—a very remarkable property, once again displaying their fascinating features.

V. CONCLUSIONS

Using a Markovian master equation approach with linear Lindblad operators, we investigated the dissipative phase-space dynamics of a one-electron quantum dot. We obtained the density matrix in coordinate representation from which an expression for the spatial decoherence parameter was derived. With numerically calculated initial values for the first and second moments of a quantum dot in a prepared state, we analyzed the time evolution of decoherence and the influence of the temperature and an external magnetic field. The phenomenological coupling to the environment was assumed to emerge from electron-phonon scattering. We found that the asymptotic decoherence strongly depends on the temperature and also on the magnetic field and the decoherence time scale is driven by environmental coupling strength, varying between a few and a few hundred picoseconds.

The model presented here has the advantage of being rather simple. The price one has to pay is, on one hand, its phenomenological nature and, on the other hand, the restriction to Markovian dynamics. Hence, the obtained results should be viewed with these limitations in mind. If, for example, one aims to investigate decoherence arising from faster processes than electron-phonon scattering, the weak-coupling limit is not necessarily valid since the dissipation

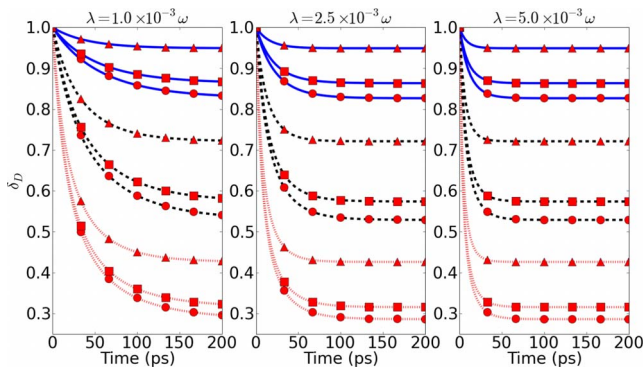


FIG. 3. (Color online) Time evolution of the decoherence degree for three different environmental coupling strengths λ . The solid curves correspond to a temperature of $T=25$ K, the dashed curves to $T=50$ K, and the dotted curves to $T=100$ K; while the different magnetic fields are indicated by symbols $B=1$ T (circles), $B=3$ T (squares), and $B=7$ T (triangles).

constant approaches the confinement strength. At the same time, the phenomenological nature also has the advantage that one is able to describe different kinds of interactions without loss of generality, just by choosing different values for the emerging constants, as long as the Markovian condition is not violated.

Further difficulties can occur, if, for example, the circular symmetry is disturbed or anharmonic effects have to be accounted for. In that case, the off-diagonal coupling constants in Eq. (12) or Eq. (19) may be nonzero and it may also be quite nontrivial to find a single decoherence parameter in this case. It should be stressed that analytical solvability is provided for a purely harmonic confinement only, while for more complex potentials even a numerical solution is not always possible since no finite system of the equations of motions can be derived.

Another conclusion we can draw from the present study is that if the temperature is very much smaller than the confinement strength ($kT \ll \hbar\omega$), spatial decoherence should not be

of significant relevance. Even at a temperature of 25 K, we see that the asymptotic decoherence is about $\delta_D(t \rightarrow \infty) \approx 0.9$. However, in some experimental setups, the temperatures are as low as $T=100$ mK and hence we can conclude that spatial decoherence practically does not occur in that case.

As for further applications of the model presented here, it should be also suited to study tunneling processes in quantum-dot molecules. Calculations on tunneling through one-dimensional parabolic potentials with dissipation described by linear Lindblad operators were, e.g., demonstrated in Refs. 65 and 66, which can be extended to the two-dimensional case.

ACKNOWLEDGMENTS

Financial support from the Göran Gustafsson Foundation and the Swedish science research council (VR) is gratefully acknowledged.

-
- ¹D. Loss and D. P. DiVincenzo, Phys. Rev. A **57**, 120 (1998).
²J. A. Folk, C. M. Marcus, and J. S. Harris, Phys. Rev. Lett. **87**, 206802 (2001).
³H. Htoon, D. Kulik, O. Baklenov, A. L. Holmes, T. Takagahara, and C. K. Shih, Phys. Rev. B **63**, 241303(R) (2001).
⁴A. Vagov, V. M. Axt, T. Kuhn, W. Langbein, P. Borri, and U. Woggon, Phys. Rev. B **70**, 201305(R) (2004).
⁵S. Sanguinetti, E. Poliani, M. Bonfanti, M. Guzzi, E. Grilli, M. Gurioli, and N. Koguchi, Phys. Rev. B **73**, 125342 (2006).
⁶F. Bernardot, E. Aubry, J. Tribollet, C. Testelin, M. Chamarro, L. Lombez, P. F. Braun, X. Marie, T. Amand, and J.-M. Gérard, Phys. Rev. B **73**, 085301 (2006).
⁷A. V. Khaetskii, D. Loss, and L. Glazman, Phys. Rev. Lett. **88**, 186802 (2002).
⁸A. Khaetskii, D. Loss, and L. Glazman, Phys. Rev. B **67**, 195329 (2003).
⁹V. N. Golovach, A. Khaetskii, and D. Loss, Phys. Rev. Lett. **93**, 016601 (2004).
¹⁰S. Vorojtsov, E. R. Mucciolo, and H. U. Baranger, Phys. Rev. B **71**, 205322 (2005).
¹¹L. Jacak, J. Krasnyj, W. Jacak, R. Gonczarek, and P. Machnikowski, Phys. Rev. B **72**, 245309 (2005).
¹²M. Thorwart, J. Eckel, and E. R. Mucciolo, Phys. Rev. B **72**, 235320 (2005).
¹³W. Zhang, V. V. Dobrovitski, K. A. Al-Hassanieh, E. Dagotto, and B. N. Harmon, Phys. Rev. B **74**, 205313 (2006).
¹⁴W. Yao, R. B. Liu, and L. J. Sham, Phys. Rev. B **74**, 195301 (2006).
¹⁵D. D. Bhaktavatsala Rao, V. Ravishankar, and V. Subrahmanyam, Phys. Rev. A **74**, 022301 (2006).
¹⁶C. Deng and X. Hu, Phys. Rev. B **73**, 241303(R) (2006).
¹⁷C. Deng and X. Hu, Phys. Rev. B **74**, 129902(E) (2006).
¹⁸W. Ben Chouikha, S. Jaziri, and R. Bennaceur, Phys. Rev. A **76**, 062303 (2007).
¹⁹Y. G. Semenov and K. W. Kim, Phys. Rev. B **75**, 195342 (2007).
²⁰J. H. Jiang, Y. Y. Wang, and M. W. Wu, Phys. Rev. B **77**, 035323 (2008).
²¹P. Stano and J. Fabian, Phys. Rev. B **77**, 045310 (2008).
²²W. Zhang, N. P. Konstantinidis, V. V. Dobrovitski, B. N. Harmon, L. F. Santos, and L. Viola, Phys. Rev. B **77**, 125336 (2008).
²³L. M. Woods, T. L. Reinecke, and A. K. Rajagopal, Phys. Rev. B **77**, 073313 (2008).
²⁴W. Yang and R. B. Liu, Phys. Rev. B **77**, 085302 (2008).
²⁵F. G. G. Hernandez, A. Greilich, F. Brito, M. Wiemann, D. R. Yakovlev, D. Reuter, A. D. Wieck, and M. Bayer, Phys. Rev. B **78**, 041303(R) (2008).
²⁶M. W. Y. Tu and W. M. Zhang, Phys. Rev. B **78**, 235311 (2008).
²⁷W. H. Zurek, Rev. Mod. Phys. **75**, 715 (2003).
²⁸E. Waltersson, E. Lindroth, I. Pilskog, and J. P. Hansen, Phys. Rev. B **79**, 115318 (2009).
²⁹A. Isar and W. Scheid, Physica A **373**, 298 (2007).
³⁰R. K. Gupta, M. Muenchow, A. Sandulescu, and W. Scheid, J. Phys. G **10**, 209 (1984).
³¹A. Sandulescu, H. Scutaru, and W. Scheid, J. Phys. A **20**, 2121 (1987).
³²Y. V. Palchikov, G. G. Adamian, N. V. Antonenko, and W. Scheid, J. Phys. A **33**, 4265 (2000).
³³P. A. Maksym and T. Chakraborty, Phys. Rev. Lett. **65**, 108 (1990).
³⁴S. M. Reimann and M. Manninen, Rev. Mod. Phys. **74**, 1283 (2002).
³⁵E. Waltersson and E. Lindroth, Phys. Rev. B **76**, 045314 (2007).
³⁶A. E. Rothman and D. A. Mazziotti, Phys. Rev. A **78**, 032510 (2008).
³⁷V. V. Dodonov and O. V. Manko, Physica A **130**, 353 (1985).
³⁸S. A. Kalandarov, Z. Kanokov, G. G. Adamian, and N. V. Antonenko, Phys. Rev. E **75**, 031115 (2007).
³⁹C. Anastopoulos and B. L. Hu, Phys. Rev. A **62**, 033821 (2000).
⁴⁰C. H. Chou, T. Yu, and B. L. Hu, Phys. Rev. E **77**, 011112 (2008).
⁴¹G. Lindblad, Commun. Math. Phys. **48**, 119 (1976).

- ⁴²R. Karrlein and H. Grabert, Phys. Rev. E **55**, 153 (1997).
- ⁴³M. R. Gallis, Phys. Rev. A **53**, 655 (1996).
- ⁴⁴Z. Haba, Phys. Rev. A **57**, 4034 (1998).
- ⁴⁵A. Isar, A. Sandulescu, and W. Scheid, Phys. Rev. E **60**, 6371 (1999).
- ⁴⁶A. Isar and W. Scheid, Phys. Rev. A **66**, 042117 (2002).
- ⁴⁷K. Dietz, J. Phys. A **37**, 6143 (2004).
- ⁴⁸H. Dekker and M. C. Valsakumar, Phys. Lett. **104A**, 67 (1984).
- ⁴⁹A. Săndulescu and H. Scutaru, Ann. Phys. **173**, 277 (1987).
- ⁵⁰G. G. Adamian, N. V. Antonenko, and W. Scheid, Nucl. Phys. A **645**, 376 (1999).
- ⁵¹G. G. Adamian, N. V. Antonenko, and W. Scheid, Phys. Lett. A **260**, 39 (1999).
- ⁵²M. C. Wang and G. E. Uhlenbeck, Rev. Mod. Phys. **17**, 323 (1945).
- ⁵³G. S. Agarwal, Phys. Rev. A **4**, 739 (1971).
- ⁵⁴E. Joos, H. D. Zeh, C. Kiefer, D. Giulini, J. Kupsch, and I. O. Stamatescu, *Decoherence and the Appearance of a Classical World in Quantum Theory* (Springer-Verlag, Berlin, 2003).
- ⁵⁵M. Schlosshauer, *Decoherence and the Quantum-to-Classical Transition* (Springer-Verlag, Berlin, 2007).
- ⁵⁶M. Morikawa, Phys. Rev. D **42**, 2929 (1990).
- ⁵⁷P. Földi, M. G. Benedict, A. Cziráj, and B. Molnár, Phys. Rev. A **67**, 032104 (2003).
- ⁵⁸H. Friedrich, *Theoretical Atomic Physics* (Springer-Verlag, Berlin, 2006).
- ⁵⁹C. deBoor, *A Practical Guide to Splines* (Springer-Verlag, Berlin, 1978).
- ⁶⁰U. Bockelmann, Phys. Rev. B **50**, 17271 (1994).
- ⁶¹A. Bertoni, M. Rontani, G. Goldoni, and E. Molinari, Phys. Rev. Lett. **95**, 066806 (2005).
- ⁶²V. N. Stavrou and X. Hu, Phys. Rev. B **72**, 075362 (2005).
- ⁶³J. I. Climente, A. Bertoni, G. Goldoni, and E. Molinari, Phys. Rev. B **74**, 035313 (2006).
- ⁶⁴W. H. Zurek, Phys. Today **44**(10), 36 (1991).
- ⁶⁵G. G. Adamian, N. V. Antonenko, and W. Scheid, Phys. Lett. A **244**, 482 (1998).
- ⁶⁶A. Isar, A. Sandulescu, and W. Scheid, Eur. Phys. J. D **12**, 3 (2000).